Elastic scattering of ^{7}Li+^{28}Si at near-barrier energies

A. Pakou,[1,*] N. Alamanos,[2] G. Doukelis,[3] A. Gillibert,[2] G. Kalyva,[4] M. Kokkoris,[5] S. Kossionides,[4] A. Lagoyannis,[1,†] A. Musumarra,[6] C. Papachristodoulou,[1] N. Patronis,[1] G. Perdikakis,[4] D. Pierroutsakou,[7] E. C. Pollacco,[2] and K. Rusek[8]

[1]*Department of Physics, The University of Ioannina, 45110 Ioannina, Greece*

[2]*DSM/DAPNIA CEA SACLAY, 91191 Gif-sur-Yvette, France*

[3]*Technical Educational Institute of Athens, 12210 Athens, Greece*

[4]*National Research Center, Demokritos, Greece*

[5]*National Technical University of Athens, Athens, Greece*

[6]*Dipartimento di Metodologie Fisiche e Chimiche per l'Ingegneria dell'Universita di Catania, Catania, Italy*

[7]*INFN Sezione di Napoli, I-80125, Napoli, Italy*

[8]*Department of Nuclear Reactions, The Andrzej Sołtan Institute for Nuclear Studies, Hoża 69, 00-681 Warsaw, Poland*

(Received 12 December 2003; published 5 May 2004)

The ^{7}Li+^{28}Si elastic scattering was studied at near-barrier energies, namely, 8, 8.5, 9, 10, 11, 13, 15, and 16 MeV, with the aim to map the real and imaginary part of the optical potential and therefore probe the threshold anomaly. Angular distributions were measured over a wide angular range of (θ_{lab}=25° to 150°) for the lower energies and of (θ_{lab}=10° to 100°) for the higher energies. The present data, together with previous ones on heavier targets (^{138}Ba and ^{208}Pb) at near barrier energies, were analyzed by using optical potentials obtained in a double-folding framework. The results were compared with previous measurements of ^{6}Li on the same targets. It was found that a striking difference occurs between the imaginary potentials of ^{6}Li and ^{7}Li, which, respectively, present an increasing and decreasing behavior approaching the barrier from higher to lower energies. On the other hand, this energy variation is not fully reflected to the real part of the potential, as it is described by dispersion relations. The strength of the real potential remains almost constant with a weak declining and uprising trend for the ^{6}Li and ^{7}Li, respectively. For a better understanding of our results, continuum-discretized-coupled-channel calculations were also performed and are discussed.

DOI: 10.1103/PhysRevC.69.054602 PACS number(s): 25.70.Bc, 24.10.Ht, 27.20.+n

I. INTRODUCTION

In the past years the phenomenon of "threshold anomaly" in the optical potential around the barrier has been well established for stable encounters [1]. It is visualized as a rapid energy variation of both the real and imaginary parts in the vicinity of the barrier, where a peak develops in the real part associated through dispersion relations with the decrease of the imaginary part as the energy is decreasing [2]. The physical origin of the effect is due to strong couplings to low-lying states in both the projectile and target, to inelastic scattering and transfer reactions.

It was suggested [2] that the same effect may not appear for weakly bound systems where coupling to breakup channels gives a repulsive contribution to the real part of the optical potential, which is almost independent of bombarding energy, while the associated imaginary potential is very small. Therefore, the dispersion relation is of no use in these circumstances. After that, several works were devoted to studies of elastic scattering in the vicinity of the barrier for weakly bound systems concerning mainly the nuclei ^{6,7}Li [3–11]. In view of the similarities of weakly bound stable systems with their associate weakly bound radioactive ones [12], such studies are of critical importance as they can indicate trends and give initiatives for studies of drip line nuclei, while the measurements can be performed by using stable beams and therefore can decongest the heavy schedule of radioactive beam facilities. In a very recent study [13,14] on the elastic scattering of ^{6}Li+^{28}Si, which was strengthened by the analysis of previous data on heavier targets into the same footing, an unusual behavior of both the real and imaginary part of the optical potential was established at near barrier energies. More explicitly, the normalization factor of the real part of the double-folding potential was found to remain almost constant till the barrier, with a slight declining trend, and presenting a reduction of ~40% similar to the one that is established for energies well above the Coulomb barrier [15]. The normalization factor of the imaginary potential was found to present an increasing trend with decreasing energy. On the other hand, a conclusion for ^{7}Li is not straightforward. From the performed studies thus far, its behavior seems to contradict that of ^{6}Li, at least in what concerns the imaginary part, which for ^{7}Li shows a rather similar trend with the one exhibited by stable systems. According to the authors of Ref. [3], for the real part of the potential a weak peak, blurred however by the scattering of the data, develops at the barrier. This peak can be described quantitatively by dispersion relations only if an assumption is made about a continuous loss of flux from the elastic scattering channel below barrier. This is not consistent however with recent α-breakup measurements [16]. Near the barrier, deviations from Rutherford scattering are mostly featureless, and thus, in order to draw stronger statements, more data are necessary in preference with light targets where the Coulomb potential is smaller. Also, data at several energies are neces-

*Corresponding author. Email address: apakou@cc.uoi.gr

†Present address: National Research Center, Demokritos, Greece.

sary to map well the potential and apply dispersion relations.

To contribute in that direction, we have undertaken the study both experimentally and theoretically of the ^{7}Li+^{28}Si elastic scattering at near-barrier energies. It should be noted that this system is studied for the first time at these energies. We report also, in the same theoretical context, the analysis of data on heavier targets while making comparisons with previous results of ^{6}Li on the same targets. The outline of this paper is as follows. In Sec. II we present experimental details and the measurements. Section III contains the theoretical analysis of present and previous data on heavier targets into a folding context. In Sec. IV our continuum-discretized-coupled-channel (CDCC) calculations are presented. In Sec. V we show the analysis of dispersion corrections to the real potential due to the energy variation of the imaginary part. Finally, in Sec. VI are the discussion and our conclusions.

II. EXPERIMENTAL DETAILS

$^{7}Li^{2+}$ and $^{7}Li^{3+}$ beams were delivered by the TN11/25 HVEC 5.5 MV Tandem accelerator of the National Research Center of Greece-Demokritos at eight bombarding energies, namely, 8, 8.5, 9, 10, 11, 13, 15, and 16 MeV. Beam currents were of the order of 30 nA. The beam impinged on a 210-μg/cm^2-thick, self-supported natural silicon target, tilted by ±45° (depending on the detector position) and the elastically scattered Li ions were detected in two solid state surface barrier detectors. One of the detectors was a telescope (the ΔE silicon detector was 10 μm thick, while the E detector was 300 μm thick) measuring the forward-angle scattering, while the other one was a thin, 20- or 25-μm-thick silicon detector measuring the backward scattering. The choice of the thickness of the backward detector was such as to allow light particles, like alphas from breakup transfer and other contaminant reactions (^{7}Li+^{12}C), to go through while Li particles stop in the detector. The alpha group was well discriminated in the forward detectors with the ΔE-E technique. The detectors were set 24 cm away from the target on a remote control rotating table. Tantalum masks were placed in front of each detector and an angular resolution of 0.7° was obtained. This angular uncertainty was estimated to increase to 1° due to the beam divergence. The subtending solid angle was 1.2×10^{-4} sr. An overall normalization was obtained at each energy by placing two monitor silicon detectors, 300 μm thick, behind the telescopes, 34 cm away from the target, fixed at ±15° on a bottom table, concentric to the top rotating one. The scattering at ±15°, concerning the present bombarding energies, can be considered as being pure Rutherford. These monitors behind the telescopes were shadowed by one of them when they were rotated between 10° to 20°. For that reason a third monitor detector was set at 40°. The scattering on this detector was found to drop from ~95% to 70% of the Rutherford scattering from the lower to the higher energies. A liquid-nitrogen cold trap close to the target holder reduced the target contamination on carbon to minimum. This was confirmed at the end of the runs in a separate Rutherford back scattering experiment [17], during which the carbon contaminant was estimated and the target thickness was established.

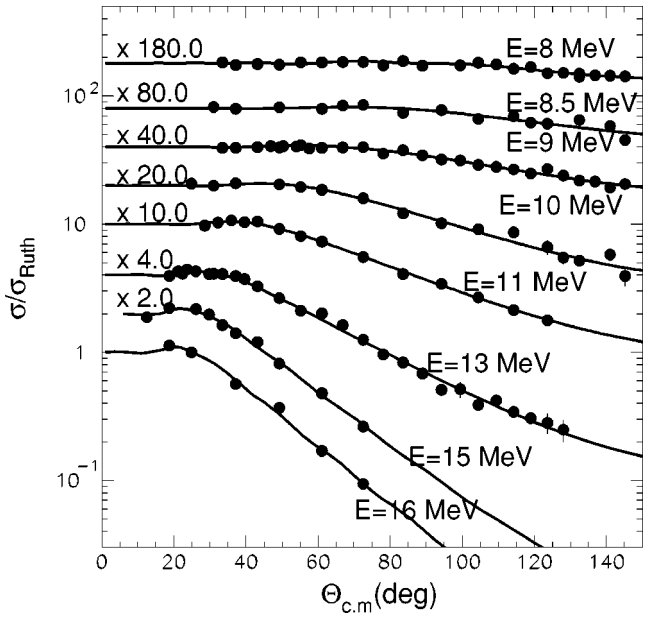

FIG. 1. Present elastic scattering data for the system ^{7}Li+^{28}Si. The statistical error was 2–6 %, while the error adopted in all our fits was 10%. The solid lines represent the best fits adopting a double-folded potential for the real and imaginary part. The normalization factors are given in Fig. 3.

Angular distributions were determined in steps of 2° to 10° depending on the energy and angular range. The data were recorded using a PC controlled acquisition system, CAMDA [18] and were analyzed off line. The results are shown in Fig. 1. Under the same conditions we also performed a ^{6}Li+^{28}Si angular distribution measurement at 13 MeV, as a test run, since our final goal was to compare results for the two weakly bound nuclei. The results are shown in Fig. 2 and show very good consistency with our previous data [13] and older ones [19].

III. THEORETICAL ANALYSIS-FOLDING FRAMEWORK

For the theoretical analysis, elastic scattering calculations were performed with the code ECIS [20]. The real part of the entrance potential was calculated within the double-folding model [21] by using the BDM3Y1 interaction developed by Khoa *et al.* [22]. The densities involved in the real double-folded potential of the present analysis were obtained from electron scattering data, adopting a three parameter Fermi model, for ^{28}Si [23], and Hartree-Fock calculations obtained by Trache *et al.* [15] for ^{7}Li. Calculations with harmonic oscillator densities and densities from phenomenological descriptions [24] for ^{7}Li did not alter the results appreciably.

The imaginary potential was assumed to be of the same radial shape as the real one and the same folded potential was adopted, but with a different normalization factor. A search was performed by using as free parameters the two normalization factors for the real and imaginary potential, N_R and N_I. The results of the best fits are shown in Fig. 3, while

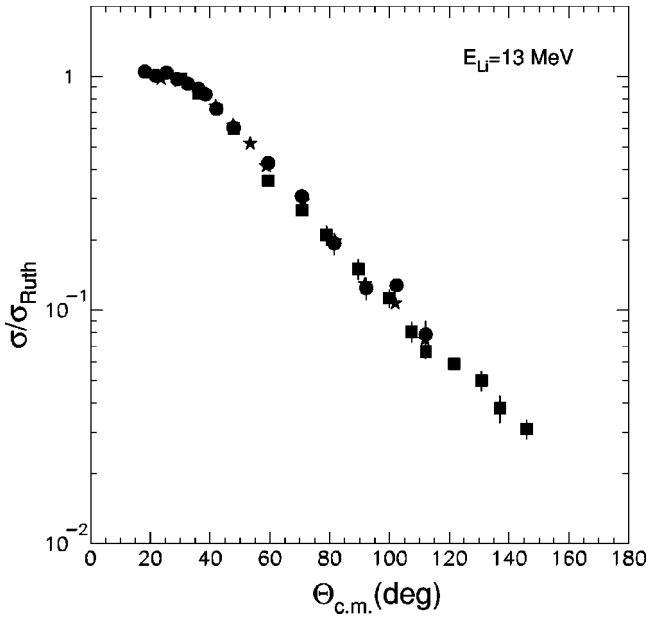

FIG. 2. Present data for ^{6}Li+^{28}Si (solid circles), from a test run, are compared with previous data designated with solid boxes [13] and solid stars [19]. The good consistency of these data gives further support to our new data for the system ^{7}Li+^{28}Si.

the deduced angular distributions are compared with the data in Fig. 1. It has to be pointed out here that we have considered it more appropriate to plot these normalization factors as a function of energy, rather than the values of the real and imaginary potential at the strong absorption radius, since for

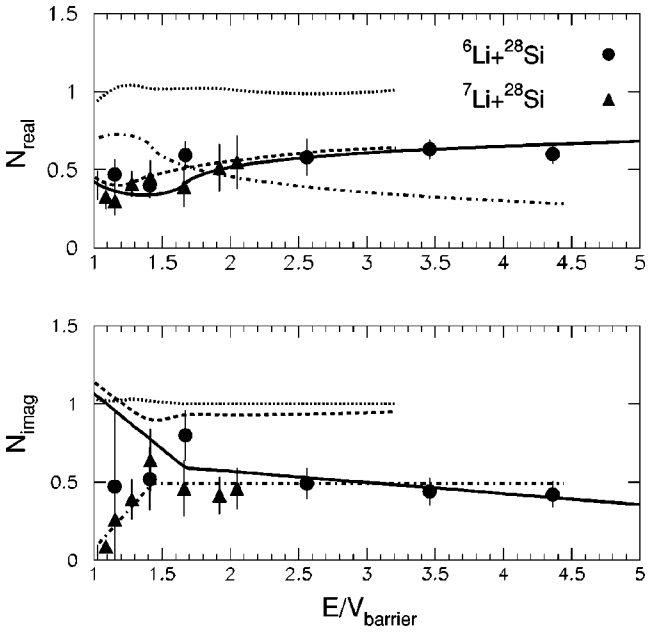

FIG. 3. Normalization factors of the real and imaginary potential for ^{6,7}Li+^{28}Si as a function of the lithium bombarding energy over barrier. Barriers were taken from previous measurements [13] as 7.8 MeV for both systems in the laboratory frame. The lines correspond to dispersion calculations (solid line and dotted-dashed line for ^{6}Li and ^{7}Li, respectively) and to CDCC calculations (dashed and dotted line for ^{6}Li and ^{7}Li, respectively).

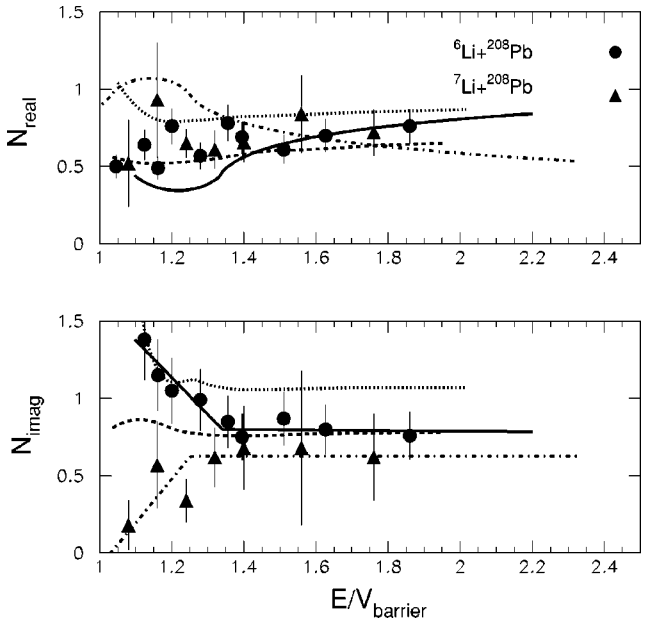

FIG. 4. Normalization factors of the real and imaginary potential for ^{6,7}Li+^{208}Pb, as a function of the lithium bombarding energy over barrier. Barriers in the laboratory were taken from previous measurements [11] as 25.84 MeV for both systems. The lines correspond to dispersion calculations (solid line and dotted-dashed for ^{6}Li and ^{7}Li, respectively) and to CDCC calculations (dashed and dotted line for ^{6}Li and ^{7}Li, respectively).

light elements the radial region of sensitivity may change with bombarding energy. Additionally, the definition of the strong absorption radius is not straightforward for weakly bound encounters. As it was pointed out in [12,25] the reduced distance of closest approach for the systems ^{6}He +^{208}Pb and ^{6,7}Li+^{28}Si is ~2.2 fm instead of ~1.65 fm for stable encounters. In Fig. 3 we also present our previous results of ^{6}Li+^{28}Si [13] analyzed under the same theoretical footing. As it is seen, no marked difference is observed for the two weakly bound nuclei. For ^{6}Li, a slight increasing trend of the imaginary potential as the energy decreases to the barrier cannot establish a different behavior from ^{7}Li due to the errors and to the lack of data points in comparison with the ^{7}Li case. On the other hand, the ^{6}Li data, as it was pointed out in [13], are also consistent with the increasing trend seen for ^{6}Li scattering on heavier targets. More data at smaller energy steps might be necessary to complement the previous ^{6}Li ones in order to obtain a more detailed mapping of the imaginary potential as was done in the present work for ^{7}Li. Complementary total reaction cross section measurements will also be valuable at that point.

To gain a more global insight into the subject, former data for the systems ^{6,7}Li+^{138}Ba [7] and ^{6,7}Li+^{208}Pb [3] were also analyzed in the same context and the results are presented in Figs. 4 and 5. A marked difference between ^{6}Li and ^{7}Li is evident at least in what concerns the energy variation of the imaginary part, where an increasing behavior is established for ^{6}Li and a decreasing one for ^{7}Li approaching the barrier from higher to lower energies. This difference is seen in a more prominent way for the Pb target, due to an existing comprehensive list of data points. On the other hand, this

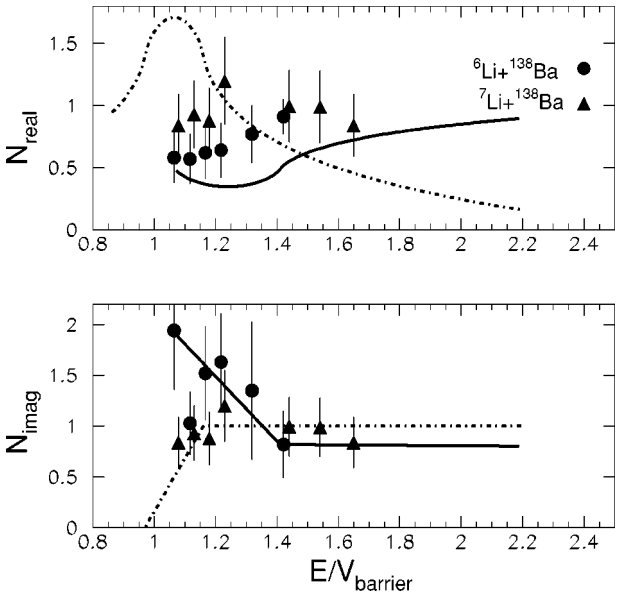

FIG. 5. Normalization factors of the real and imaginary potential for ^{6,7}Li+^{138}Ba, as a function of the lithium bombarding energy over barrier. Barriers were taken as 19.7 MeV in the laboratory system for both systems. The lines correspond to dispersion calculations (solid line and dotted-dashed for ^{6}Li and ^{7}Li, respectively).

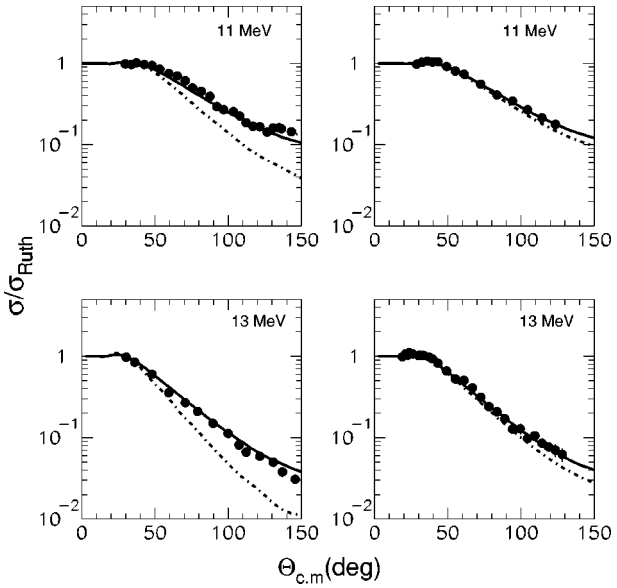

FIG. 6. Elastic scattering data at 11 and 13 MeV for the systems ^{6}Li+^{28}Si (left column) and ^{7}Li+^{28}Si (right column) are compared with CDCC (solid line) and one channel calculations (dotted-dashed line). As it is seen, the effect of breakup is more substantial for ^{6}Li scattering than for ^{7}Li scattering and for higher energies than for lower energies.

sharp energy variation of the imaginary part is not reflected in the real part of the potential, which shows for both weakly bound nuclei an almost constant behavior. We note however that for the scattering of ^{6}Li a weak declining trend develops, seen mainly on the Si and Ba target data, while for the scattering of ^{7}Li a weak uprising trend develops instead, mainly seen for the Pb data. In both cases the $W(E)$ energy variation is significant, a fact that justifies the use of dispersion relations. The dispersion contribution to the real part of the optical potential due to the $W(E)$ variation is discussed in Sec. V.

IV. THEORETICAL ANALYSIS-CDCC CALCULATIONS

These calculations were performed using version FRXP.18 of the code FRESCO [26] for the system ^{6}Li+^{28}Si at the energy range E_{lab}=7.5 to 25 MeV and for the system ^{7}Li+^{208}Pb at the energy range E_{lab}=27 to 52 MeV. The model used was very close to that of Refs. [8,27]. It was assumed that the nucleus ^{6}Li (^{7}Li) has a two-body $\alpha+d$ ($\alpha+t$) cluster structure. Couplings between resonant and nonresonant cluster states corresponding to α-d (α-t) relative orbital angular momentum $L=0,1,2$ ($L=0,1,3$) were included. For ^{7}Li the excitation to first excited state and ground state reorientation was also taken into account The continuum above the $^6\mathrm{Li}\rightarrow\alpha+d$ ($^7\mathrm{Li}\rightarrow\alpha+t$) breakup theshold was discretized into momentum bins. The width of most of the bins was set to $\Delta k=0.26$ fm^{-1} for ^{6}Li and to $\Delta k=0.25$ fm^{-1} for ^{7}Li. In the presence of the resonant states the binning schemes were suitably modified in order to avoid double counting. Upper limits of the continuum states were taken as 10.6 and 9.3 MeV for the ^{6}Li and ^{7}Li on silicon, respectively, at 13 MeV beam energy. These limits were reduced for the lower energies according to the appropriate value of $E_{c.m.}$ of the system. All the diagonal and coupling potentials were generated from empirical α+ target, d+ target, and t+ target optical model potentials for the corresponding target nucleus by means of the single-folding technique. For the ^{208}Pb target these potentials were the same as in Ref. [27], while for the ^{28}Si target the corresponding potentials were adopted from Refs. [28–30].

In the above context, angular distributions with one channel calculations and CDCC calculations are compared with some of the data in Fig. 6 (^{6,7}Li+^{28}Si at 11 and 13 MeV). The agreement of the data with the calculations is in general good. It is obvious that the CDCC improvement due to the breakup is more substantial for the ^{6}Li scattering than for the ^{7}Li scattering. Also, it is more substantial at higher energies than at lower energies. Furthermore, to make comparisons in terms of the potentials we plot in Figs. 3–5 ratios of the quantities V_{eff}/V_{bare} ($V_{eff}=V_{bare}+V_{polarization}$) at the strong absorption radius (R_s). We have to point out here that we make such comparisons with some caution, since as we have stated before in Sec. III, for light elements the radial region of sensitivity changes with absorption radius for light elements and additionally the reduced distance of closest approach for some weakly bound nuclei is larger than expected for stable encounters. The ratios V_{eff}/V_{bare} for the systems ^{6,7}Li+^{28}Si are plotted at the strong absorption radius R_s=10.6 fm=2.2$\times(A_1^{1/3}+A_2^{1/3})$ fm according to our findings in [12] for the distance of closest approach. For the systems ^{6,7}Li+^{208}Pb we plot the potentials at a distance R_s=12.4 fm=1.6$\times(A_1^{1/3}+A_2^{1/3})$ fm used by previous authors, since we have no evidence for the moment about the distance of closest approach for these systems. In principle, the CDCC calculations fail to reproduce the data. In more detail, however, the following

remarks can be made. For the system ^{6}Li+^{28}Si, the real part of the potential follows the data well, while the imaginary part shows a qualitative agreement with the trend but not with the strength. For the system ^{7}Li+^{28}Si, the calculations for both the imaginary and real part are well off the data. For the system ^{6}Li+^{208}Pb, we also have a good agreement with the real potential data but not with the imaginary potential one. Finally, for the system ^{7}Li+^{208}Pb the calculations for both the imaginary and real part are well off the data.

The general conclusion drawn from these results is that more reaction channels, like the *t*-transfer channel that is expected to be very strong for ^{7}Li+^{28}Si, have to be explicitly taken into account in model calculations. As it becomes more and more evident, the competition between breakup and transfer and/or other reaction processes varies with energy and target mass number [14] and therefore affects in a unique way each scattering system. It was shown in [14], that for ^{6}Li+^{28}Si the ratio of the predicted breakup cross section to the total alpha production is very small (of the order of 8% for $E_{\mathrm{beam}}=13$ MeV). On the other hand, test calculations performed in this work for ^{7}Li+^{28}Si show that this ratio is almost zero. For the lead target the role of breakup is more pronounced since the ratio of the breakup cross section to the total α production is much larger [14,16] (of the order of 25% for $E_{\mathrm{beam}}=33$ MeV). However, even in that case, breakup is not enough to describe the singularities of the potential at barrier. Moreover, the effect of reorientation and excitation to low-lying states, in the case of the ^{7}Li scattering, is indeed impressive concerning breakup cross sections (the breakup cross section can be increased by a factor of 5). However, this effect is not enough to give any change to the potential energy trend since breakup does not seem to be the major process at barrier for none of the two weakly bound nuclei.

V. DISPERSION CALCULATIONS

Elastic scattering differential cross sections can be well reproduced, introducing an effective interaction or optical potential, and thus reducing the many-body problem to a one-body problem.

$$U(r;E) = V(r;E) + iW(r;E), \tag{1}$$

where V and W are the real and imaginary parts related through the following dispersion relation [2]:

$$V(r;E) = V_0(r;E) + \Delta V(r;E),$$
$$\Delta V(r;E) = \frac{P}{\pi}\int_0^{\infty} \frac{W(r;E')}{E'-E}dE', \tag{2}$$

where ΔV is an attractive polarization potential. Although the behavior of W at high energies is not known, this has little effect on the shape of $\Delta V(E)$ at low energies. Therefore, instead of relation (2) we can use the dispersion relation in a subtracted form, normalizing V_0 at some convenient energy E_s,

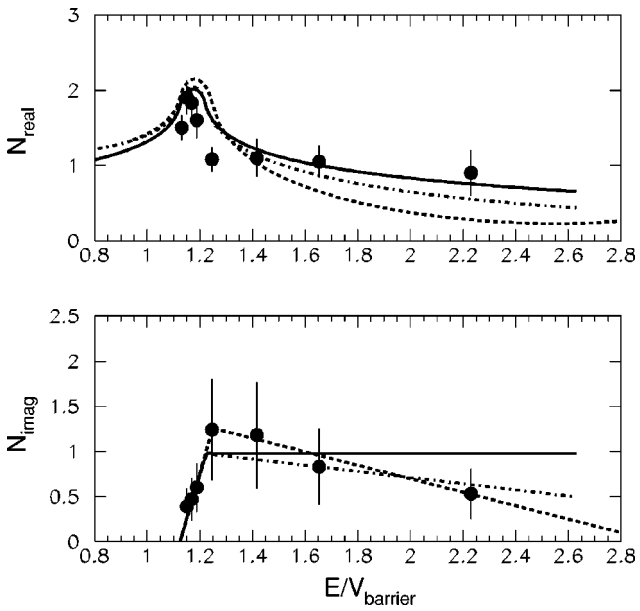

FIG. 7. Normalization factors of the real and imaginary potential for ^{12}C+^{209}Bi as a function of the carbon bombarding energy over barrier. The barrier was taken as 52.8 MeV in the laboratory frame. The lines correspond to dispersion calculations. It is obvious that the dispersion correction follows the data adequately well, giving further support to our systematic analysis made in this work for the weakly bound systems.

$$V(r;E) = V_0(r;E_s) + \frac{P}{\pi}(E-E_s)\int_0^{\infty} \frac{W(r;E')}{(E'-E_s)(E'-E)}dE'. \tag{3}$$

In the following, we will demonstrate the effect of the dispersive coupling via relation (3) for stable and weakly bound systems by use of the simple linear segments model suggested in [2] for describing $W(r,E)$.

To establish our method, we started our calculations by treating elastic scattering data for stable encounters, namely, data of the ^{12}C+^{209}Bi system [31], in the same theoretical folding context (Sec. III) applied for the systems ^{6,7}Li+^{28}Si, ^{6,7}Li+^{138}Ba, and ^{6,7}Li+^{208}Pb. The obtained energy variation of the optical potential, real and imaginary part, is displayed in Fig. 7. A threshold anomaly of the conventional type is obvious. To apply the dispersion correction, we have chosen two linear segments (solid line) for representing the energy variation of the imaginary potential. To demonstrate the sensitivity of the choice of linear segments, we have also considered two additional lines with different slopes (dashed and dotted-dashed lines in Fig. 7). As it is seen the variation of the slope of the second segment has an effect on the slope of the line describing the real potential after the barrier (a variation on the slope of the first segment line would effect the width of the peak of the real potential at the barrier). In principle, as it can be seen from Fig. 7, the dispersive effect on the real part due to the energy variation of the imaginary part describes adequately well the data.

In the above context we have estimated the dispersive correction for the systems ^{6,7}Li+^{28}Si, ^{6,7}Li+^{138}Ba, and

^{6,7}Li + ^{208}Pb [13,31,5]. We have also applied here the two-segment model. For ^{6}Li + ^{28}Si the increasing behavior of the imaginary potential is not well mapped due perhaps to the few existing measurements at barrier. Therefore, we have adopted the linear segments that were consistent with the imaginary potential data of the heavier targets. For ^{7}Li the imaginary potential was mapped adequately well. Two lines were fitted to the data. The line of the second segment was assumed constant, although a declining tendency of the data with increasing energy was noticed. This was preferred because a slope of this line had a declining effect on the real part of the potential at high energies not consistent with the data. The obtained dispersion corrections to the real part are plotted in Fig. 3 with the dotted-dashed and solid lines for ^{7}Li and ^{6}Li, respectively. In the same spirit, dispersion corrections to the real potential according to the $W(E)$ variation were applied for the systems ^{6,7}Li + ^{138}Ba and ^{6,7}Li + ^{208}Pb.

Obviously, the striking difference of the opposite behavior for the imaginary potential seen for ^{7}Li and ^{6}Li is also represented in the dispersion correction of the real part of their potential, which in the first case is seen as a positive peak while in the second as a negative peak. Indeed for ^{6}Li there is a declining tendency of the real potential data around the barrier that is more evident for Si and Ba targets and an uprising tendency for ^{7}Li data evident for the Pb target. However, in principle, for both weakly bound nuclei ^{6}Li and ^{7}Li the dispersion correction to the real potential is very weakly followed by the data mostly on a qualitative basis, since they present a more constant behavior. This, as was suggested in [13], may indicate an energy dependence of the breakup polarization potential in the presence of the anomaly, which as it is repulsive in nature may smooth out the attractive polarization term due to the anomaly. More elaborate theoretical calculations are necessary to enlighten further this point.

VI. SUMMARY AND CONCLUSIONS

We have performed new measurements on ^{7}Li + ^{28}Si elastic scattering at several near-barrier energies. The results were analyzed in a double-folding model by using the BDM3Y1 interaction. Previous data of ^{6}Li + ^{28}Si, ^{6,7}Li + ^{138}Ba, and ^{6,7}Li + ^{208}Pb were also considered in the same theoretical framework, in order to draw meaningful comparisons.

It was found that in general the trend of the imaginary potential for ^{7}Li strongly contradicts that of ^{6}Li. In the first case, the potential presents a decreasing trend approaching the barrier from the higher to lower energies exactly in the same way as it does for stable encounters, while in the second case an increasing trend is observed. However, in the case of ^{6,7}Li + ^{28}Si this differentiation is not so obvious as the ^{6}Li data do not contradict either the increasing trend followed by the ^{6}Li scattering data on heavier targets or the ^{7}Li scattering data on the same target. This similarity of the behavior of the potentials for the ^{6}Li and ^{7}Li scattering on Si may be not accidental and due to the quoted errors or the few existing data points around the barrier; it may indeed be due to a more systematic behavior of the scattering of weakly bound nuclei on lighter targets. This controversy should be further explored with new measurements at smaller energy steps around the barrier for the ^{6}Li case and complementary total reaction cross measurements. Furthermore, for all targets and both weakly bound nuclei ^{6}Li and ^{7}Li, the sharp variation of the imaginary potential is not reflected in the real part of the potential as ispredicted by dispersion relations. The real part of the potential for the ^{7}Li scattering remains almost constant with a very weak peak seen only for the Pb target data. The real part of the ^{6}Li potential remains also almost constant with a very weak decreasing trend seen mostly for the Si and Ba data.

In conclusion, an anomalous behavior for both the real and imaginary part of the optical potential develops for the weakly bound nuclei ^{6,7}Li in the vicinity of the barrier, which in total contradicts the conventional threshold anomaly applied to stable systems. This behavior may be described only qualitatively by dispersion relations. The almost constant behavior of the real part of the potential, which does not reflect the sharp energy variation of the imaginary one, raises several questions. One may seek answers to an energy dependence of the breakup polarization potential in the presence of a conventional threshold anomaly for ^{7}Li + ^{28}Si and a new type of anomaly for ^{6}Li + ^{28}Si. The polarization potential due to breakup becomes more repulsive and compensates the attractive term of the polarization potential due to threshold anomaly, leading to a rather constant real potential in the vicinity of the barrier. Furthermore, CDCC calculations show that breakup is more important for ^{6}Li than ^{7}Li but still not enough to explain the potential at barrier. In the CDCC context, the different behavior between the ^{6}Li and ^{7}Li potential was not explained taking into account differences of the two nuclei concerning the reorientation and excitation to the first excited state of ^{7}Li. A key issue for resolving the subject will be the consideration of the competition between breakup and transfer for the scattering of ^{6}Li and ^{7}Li on light and heavy targets. This point has to be explored in detail, both experimentally and theoretically, to interpret the observed differentiations.

ACKNOWLEDGMENTS

We would like to warmly acknowledge John P. Greene from the Argon Laboratory, for providing the silicon targets. Also, we are indebted to Dr. N. Nicolis and A. Spirou for assisting in the setup of a preliminary experiment. This work was partially financed under the project "PYTHAGORAS" of the Hellenic Ministry of Development.

[1] G. R. Satchler, Phys. Rep. **199**, 147 (1991).
[2] C. Mahaux, H. Ngo, and G. R. Satchler, Nucl. Phys. A **449**, 354 (1986).
[3] N. Keeley *et al.*, Nucl. Phys. A **571**, 326 (1994).
[4] M. A. Tiede, D. E. Trcka, and K. W. Kemper, Phys. Rev. C **44**, 1698 (1991).
[5] N. Keeley and K. Rusek, Phys. Rev. C **56**, 3421 (1997).
[6] I. Martel *et al.*, Nucl. Phys. A **582**, 357 (1995).
[7] A. M. M. Maciel *et al.*, Phys. Rev. C **59**, 2103 (1999).
[8] G. R. Kelly *et al.*, Phys. Rev. C **63**, 024601 (2000).
[9] N. Keeley and K. Rusek, Phys. Lett. B **427**, 1 (1998).
[10] N. Keeley and K. Rusek, Phys. Rev. C **66**, 044605 (2002).
[11] K. O. Pfeiffer, E. Speth, and K. Bethge, Nucl. Phys. A **206**, 545 (1973).
[12] A. Pakou, 13th Panhellenic Symposium of the Hellenic Nuclear Physics Society, 29–30 May 2003.
[13] A. Pakou *et al.*, Phys. Lett. B **556**, 21 (2003).
[14] A. Pakou *et al.*, Phys. Rev. Lett. **90**, 202701 (2003).
[15] L. Trache *et al.*, Phys. Rev. C **61**, 024612 (2000); (private communication).
[16] C. Signorini *et al.*, Phys. Rev. C **67**, 044607 (2003).
[17] M. Kokkoris (private communication).
[18] CAMDA: Camac Data Acquisition System; H. Steltzer (private communication). E-mail: h.steltzer@gsi.de
[19] J. E. Poling, E. Norbeck, and R. R. Carlson, Phys. Rev. C **13**, 648 (1976).
[20] J. Raynal, Phys. Rev. C **23**, 2571 (1981).
[21] G. R. Satchler and W. G. Love, Phys. Rep. **55**, 183 (1979).
[22] D. T. Khoa *et al.*, Phys. Lett. B **342**, 6 (1995).
[23] H. D. De Vries, C. W. Jager, and C. De Vries, At. Data Nucl. Data Tables **14**, 479 (1974).
[24] C. W. Glover, R. I. Cutler, and K. W. Kemper, Nucl. Phys. A **341**, 137 (1980).
[25] B. T. Kim *et al.*, Phys. Rev. C **65**, 044607 (2002); **65**, 044616 (2002).
[26] I. J. Thompson, Comput. Phys. Rep. **7**, 167 (1988).
[27] N. Keeley and K. Rusek, Phys. Lett. B **427**, 1 (1998).
[28] H. Lacek and U. Strohbusch, Z. Phys. **A233**, 101 (1970).
[29] W. Whur, A. Hofmann, and G. Philipp, Z. Phys. **A269**, 365 (1974).
[30] P. Schwandt *et al.*, Phys. Rev. C **26**, 369 (1982).
[31] S. Santra *et al.*, Phys. Rev. C **60**, 034611 (1999).